Identification of the clinical value and biological effects of TTN mutation in liver cancer

ZHIXUE ZHANG[1-3*], YATING SUN[1-3*], ZHIRUI ZENG[1-3], DAHUAN LI[1,2], WENPENG CAO[4], SHAN LEI[1,2] and TENGXIANG CHEN[1,2]

[1]Department of Physiology, School of Basic Medical Sciences, Guizhou Medical University, Guiyang, Guizhou 550009, P.R. China; [2]Transformation Engineering Research Center of Chronic Disease Diagnosis and Treatment, Guizhou Medical University, Guiyang, Guizhou 550009, P.R. China; [3]Guizhou Provincial Key Laboratory of Pathogenesis and Drug Research on Common Chronic Diseases, Guizhou Medical University, Guiyang, Guizhou 550009, P.R. China; [4]Department of Anatomy, School of Basic Medicine, Guizhou Medical University, Guiyang, Guizhou 550009, P.R. China

Received November 12, 2024; Accepted March 11, 2025

DOI: 10.3892/mmr.2025.13530

Abstract. Liver cancer, a malignant tumor of the digestive system, is a leading cause of cancer-related mortality globally. Numerous genetic mutations associated with tumorigenesis have been identified, stemming from genomic instability. However, the clinical implications and therapeutic relevance of these mutations remain poorly understood. The present study evaluated the prognostic significance of titin (TTN) mutations in liver cancer by analyzing the mutation landscape of liver cancer tissues from The Cancer Genome Atlas (TCGA) database. The association between TTN mutations and drug susceptibility was subsequently examined using the OncoPredict algorithm and Cell Counting Kit-8 (CCK-8) assays. Furthermore, the impact of TTN mutations on hepatoma cell biology both *in vivo* and *in vitro* were assessed by reverse transcription-quantitative PCR, protein stability assays, colony formation assays, tumor spheroid formation assays and subcutaneous tumor transplantation in BALB/c nude mice. Genetic analysis of the TCGA database revealed that TTN mutations are among the most frequent mutations in liver cancer. Patients with TTN mutations exhibited worse prognoses compared with those with the wild-type allele. The OncoPredict algorithm and CCK-8 assays revealed that TTN mutations are associated with altered drug sensitivity, particularly to GSK1904529A, nilotinib, 5-fluorouracil (5-FU) and sapitinib. Additionally, TTN mutations were shown to enhance TTN protein stability, decrease intracellular ferrous ion levels and significantly decrease liver cancer sensitivity to 5-FU both *in vitro* and *in vivo*. The findings indicated that TTN mutations increase protein stability and lower intracellular ferrous ion levels, thereby suppressing ferroptosis and contributing to resistance to 5-FU in hepatoma cells. These results suggest that TTN mutations are associated with poor prognosis in liver cancer and could serve as a predictive biomarker for liver cancer progression, prognosis and drug resistance.

Correspondence to: Professor Tengxiang Chen or Dr Shan Lei, Department of Physiology, School of Basic Medical Sciences, Guizhou Medical University, Administrative Building, 9 Beijing Road, Guiyang, Guizhou 550009, P.R. China
E-mail: txch@gmc.edu.cn
E-mail: leishan@gmc.edu.cn

*Contributed equally

Key words: liver cancer, titin, mutation, clinical value, resistant

Introduction

Liver cancer, the predominant histological type of liver malignancy, accounts for the majority of global liver cancer diagnoses and mortalities (1). In total, >50% of the reported liver cancer cases worldwide occur in China (2). Despite advances in medical technology, including surgery, ablation therapy, liver transplantation, radiation therapy, interventional therapy, immunotherapy and systemic treatment options (3,4), the prognosis remains suboptimal due to the low rates of operability, transplantation and frequent recurrence (5). Furthermore, drug resistance in liver cancer continues to pose a considerable challenge. Numerous clinical studies are focused on overcoming this resistance (6-10). Hence, there is a need to identify novel diagnostic and therapeutic targets, as well as biomarkers to enhance treatment efficacy and overcome drug resistance in liver cancer.

Genomic instability is a key factor in cancer, contributing to the accumulation of mutations in tumor suppressor genes and oncogenes (11). Several of these genetic mutations serve as key features of cancer and prognostic biomarkers, such as isocitrate dehydrogenase mutations in glioma and chondrosarcoma (12), titin (TTN) mutations in melanoma, EGFR mutations in non-small cell lung cancer (NSCLC) and TP53 mutations in breast, ovarian, small cell lung cancer and NSCLC (13,14). Genetic mutations can lead to DNA repair deficiencies, altered

protein conformations, dysregulated tumor growth and proliferation, as well as resistance to chemotherapeutic agents (15,16). In liver cancer, previous studies linked tumor initiation and progression to genomic mutations that impact tumor cell proliferation, invasion, metastasis and drug resistance (17,18). The progression of liver cancer is influenced by a variety of factors, including radiation exposure, genetic mutations and epigenetic or transcriptional variations. Sequencing of human liver tumors has revealed potential driver gene mutations and key carcinogenic pathways in liver cancer (19).

The TTN gene, the largest in the human genome with 363 exons, encodes a considerable amount of myosin in striated muscle. Due to its large molecular size, complexity and plasticity, TTN is particularly susceptible to dysregulation and mutations within this gene can lead to myosin dysfunction and associated diseases (20,21). TTN mutations have been associated with various skeletal and cardiomyopathies, with truncated TTN variants primarily associated with dilated cardiomyopathy (22). TTN mutations also carry out a role in cancer development and resistance (23). TTN mutations have been frequently observed across diverse tumor types, including ocular surface squamous neoplasia, lung squamous cell carcinoma, ovarian serous cystadenocarcinoma and thyroid cancer (24,25). The impact of TTN mutations varies between different types of cancer; for instance, patients with wild-type TTN exhibit markedly longer overall survival compared with patients with TTN mutations in immunotherapy for endometrioid endometrial carcinoma and melanoma, positioning TTN mutations as an independent marker of poor prognosis (26). By contrast, TTN mutations in other solid tumors, such as lung squamous cell carcinoma and gastric cancer, are associated with improved chemotherapy responses and longer overall survival (27-29). Despite these findings, the landscape and implications of TTN mutations in liver cancer remain largely unexplored. Therefore, the present study aimed to investigate the relationship between TTN mutations and liver cancer, with a particular focus on mechanisms of drug resistance.

Materials and methods

Acquisition of somatic cell mutation spectrum and mutation analysis. RNA-sequencing (seq), microRNA (miR/miRNA)-seq, somatic mutation and clinical data from 274 patients with liver cancer in The Cancer Genome Atlas (TCGA; accession no. TCGA-LIHC; portal.gdc.cancer.gov/) cohort were obtained. Somatic mutation data were analyzed using the 'maftools' R package (version 2.18.0; bioconductor.org/packages/release/bioc/html/maftools.html) to calculate the frequency of variant classifications in liver cancer tissues and to determine the distribution of different variant gene types. Somatic variant profiles of liver cancer tissues were detected using the VarScan algorithm (30), and the top 10 most frequently mutated genes in liver cancer were visualized. A forest plot was generated to display the hazard ratio (HR) and P-value for each mutation, categorizing patients into wild-type and mutated groups.

Acquisition and analysis of gene expression profiles and identification of differentially expressed genes (DEGs). RNA-seq profiles from TCGA liver cancer cohort were downloaded, and the matrix was normalized using the limma package (version 3.6.4; bioconductor.org/packages/release/bioc/html/limma.html). Probe names were converted to gene names prior to analysis. Based on the negative binomial distribution model, edgeR is able to model gene expression count data more accurately, thereby improving the accuracy of differential expression analysis (31). Differential gene expression analysis was carried out using edgeR (version 3.44.0; bioconductor.org/packages/release/bioc/html/edgeR.html) between liver cancer tissues with TTN mutations and wild-type controls. DEGs were defined as genes with a $\log_2$ fold change ≥1 and $P<0.05$.

Functional enrichment analysis. Functional annotation and visualization of the DEGs was carried out using the DAVID Bioinformatics Resources (david.ncifcrf.gov/), enabling the identification of enriched Kyoto Encyclopedia of Genes and Genomes (KEGG; kegg.jp/) pathways and Biological Process (BP) categories. It not only provides rapid access to a variety of heterogeneous annotation data in a centralized location, but also enriches the bio-informative level of individual genes. By using Benjamini-Hochberg multiplex testing, adjust P-values to control False Discovery Rate (FDR), terms with $P<0.05$ were considered to indicate a statistically significant difference and a bubble plot was used to visualize the top five terms.

Drug sensitivity calculation. In vivo drug responses to 198 drugs in patients with liver cancer were predicted using the OncoPredict R package (version 1.2; URL: cran.r-project.org/web//packages/oncoPredict/index.html) (32). This package calculates drug scores by fitting the gene expression matrix of each liver cancer sample into the gene expression matrix of cancer cell lines from the Broad Institute's Cancer Cell Line Encyclopedia (CCLE; portals.broadinstitute.org/ccle-legacy/home). The corresponding half-maximal inhibitory concentration (IC_{50}) for each drug was determined. A higher drug score indicates greater drug resistance (32). Drug scores between patients with liver cancer exhibiting wild-type and mutant genes were compared using unpaired t-test, with $P<0.05$ considered to indicated a statistically significant difference.

Reverse transcription-quantitative PCR (RT-qPCR). Total RNA was extracted from $5x10^6$ liver cancer cells (SNU182, HuH7 and JHH7 from Procell Life Science & Technology Co., Ltd.; HepG2, Hep3B and Li7 cells were purchased from EIAab Group.) using the Total RNA Extraction Kit (Tiangen Biotech Co., Ltd.). According to the manufacturer's protocol, the Rever Tra Ace qPCR RT Master Mix (cat. no. RR037A; Takara Bio Inc.) was used to reverse transcribe total RNA into complementary DNA (cDNA). RT-qPCR was carried out using a real-time PCR instrument (cat. no. 12011319; CFX Opus 96 Real-Time PCR System), and relative expression was calculated using the $2^{-\Delta\Delta Cq}$ method (33). GAPDH was used as a loading control. The primers used were as follows: GAPDH, forward primer 5'-GTCTCCTCTGACTTCAACAGCG-3', and reverse primer 5'-ACCACCCTGTTGCTGTAGCCAA-3', TTN forward primer 5'-CCCCATCGCCCATAAGACAC-3', and reverse primer 5'-CCACGTAGCCCTCTTGCTTC-3'. The thermocycling conditions were as follows: Initial denaturation at 95.0˚C for 30 sec, followed by 40 cycles of 95.0˚C for 5 sec, 62.0˚C for 30 sec and 67.5˚C for 5 sec.

Cell culture and knockdown or overexpression of TTN. Liver cancer cell lines SNU182, HuH7 and JHH7 were obtained from Procell (Procell Life Science & Technology Co., Ltd.), while HepG2, Hep3B and Li7 cells were purchased from EIAab Group. According to mutation data from the CCLE database, JHH7, HepG2 and Li7 exhibit TTN mutations, whereas HuH7, Hep3B and SNU182 have wild-type forms of TTN. The authenticity of all cell lines used in the present study has been confirmed by STR analysis. All cell lines were cultured in Dulbecco's Modified Eagle Medium (DMEM; Gibco; Thermo Fisher Scientific, Inc.) supplemented with 10% fetal bovine serum (Gibco, Thermo Fisher Scientific, Inc.) at 37˚C and 5% CO_2.

TTN overexpression was induced via transfection with pcDNA3.1(+) plasmids (Shanghai GeneChem Co., Ltd.) using Lipofectamine 2000 (Thermo Fisher Scientific, Inc.). Empty vector was used as a negative control. Transfection was performed at 37˚C, 5% CO_2 incubator for 4-6 h and switch to fresh complete medium. After 48 h, the expression level of TTN protein was detected by Western blot to verify the overexpression effect.

Stable TTN knockdown was achieved through transduction with TTN-targeting lentivirus (iGene Biotechnology Co., Ltd.). Using a second-generation lentiviral generation system, lentiviral vector plasmids (10 μg), packaging plasmids, and envelope plasmids were co-transfected into HEK293T cells (Procell Life Science & Technology Co., Ltd.) at 50-70% confluence (4:3:1), incubated at 37˚C for 6-8 h, and then replaced with fresh complete medium. Viral supernatants were collected 48 h after transfection and viral particles were collected by ultracentrifugation (4˚C, 50,000 g, 2 h). JHH7 and HepG2 cells (50-60% confluence, lentiviral particles (MOI: 20) were added to the cell culture medium along with polybrene (5 μg/ml) and after 24 h of incubation at 37˚C, 5% CO_2 incubator, they were replaced with fresh complete medium. 48 h after transfection, puromycin (1 μg/ml; cat. no. A1113803; Thermo Fisher Scientific, Inc.) was added for 1 weeks of screening, followed by a maintenance culture using puromycin at a concentration of 0.5 μg/ml. Western blot was used to measure the expression level of TTN protein to verify the knockdown effect. All shRNAs (Shanghai Genechem Co., Ltd.) used are as follows for the sense (SS) and antisense strands (AS): sh-NC SS sequence 5'-TTCTCCGAACGTGTC ACGT-3', and AS sequence 5'-ACGTGACACGTTCGGAGA A-3'; sh1-TTN SS sequence GGTTGTTTATGTTATGTTA, and AS sequence TAACATAACATAAACAACC; sh2-TTN SS sequence GCTTGTTACTAATATAATA, and AS sequence TATTATATTAGTAACAAGC; sh3-TTN-SS sequence CAC AGAAGTTAGAGTTCAA, and AS sequence TTGAACTCT AACTTCTGTG.

Western blotting. Total protein was extracted from liver cancer cells using phenylmethanesulfonyl fluoride (1:100) in high-strength RIPA lysis buffer (Sangon Biotech Co., Ltd.). The protein concentration was determined using a BCA protein assay. SDS-PAGE electrophoresis was carried out using 12% gels (20 μg/lane), first at 80 V for 30 min and then at 120 V for 90 min. Proteins were transferred to a 0.45 μm polyvinylidene fluoride membrane for 90 min at 300 mA. The membrane was blocked with 5% skim milk powder for 1 h at room temperature, followed by overnight incubation at 4˚C with primary antibodies against GAPDH (1:5,000; cat. no. AB-2937024; Abmart Pharmaceutical Technology Co., Ltd.) and TTN (1:2,000; cat. no. H00007273-M09; Thermo Fisher Scientific, Inc.). After washing with TBS with 0.1% Tween-20, the membrane was incubated with HRP-conjugated goat anti-rabbit IgG (H+L) (1:10,000; cat. no. SA00001-2; Proteintech Group, Inc.) or HRP-conjugated Goat Anti-Mouse IgG (H+L) (1:10,000; cat. no. SA00001-1; Proteintech Group, Inc.) for 2 h at room temperature. The membrane was then treated with enhanced chemiluminescence (ECL; Omni-ECL™, Shanghai Epizyme Biotech Co., Ltd.) solution for ~1 min, followed by imaging using Tanon 5200 automatic chemiluminescence image analysis system. All experiments were carried out in triplicate as previously described (34). Optical density analysis was performed using ImageJ version 1.53t software (National Institutes of Health).

Protein stability assay. Liver cancer cells were cultured to 50-70% confluence, the old medium was removed and a fresh medium containing cycloheximide (CHX; cat. no. S7418; Selleck Chemicals) with a final concentration of 1.0 μM was added at 37˚C and 5% CO_2, cells were collected at 0, 1, 2, 3 and 4 h and protein was extracted, and the expression of TTN was detected by western blotting.

Detection of cell proliferation and viability. Cell viability was assessed using the Cell Counting Kit-8 (CCK-8; Shanghai Yeasen Biotechnology Co., Ltd.). Cells were seeded at a density of $4x10^3$ cells/well in a 96-well plate and incubated at 37˚C with 5% CO_2. Once cells adhered, Nilotinib (cat. no. HY-10159; 0.00, 0.62, 1.25, 2.50, 5.00, 10.00 and 20.00 μM), GSK1904529A (cat. no. HY-10524; 0.000, 0.031, 0.062, 0.125, 0.250, 0.500 and 1.000 μM), 5-Fluorouracil (5-FU; cat. no. HY-90006; 0.00, 0.62, 1.25, 2.50, 5.00, 10.00 and 20.00 μM) and Sapitinib (cat no. HY-13050; 0.0, 0.5, 1.0,2.0, 4.0, 8.0 and 16.0 nM) were added to the wells for 48 h. All drugs were purchased from MedChemExpress. After treatment, the culture medium containing the drug was discarded, and 100 μl of DMEM containing 1/10 of the CCK-8 reagent (Shanghai Yeasen Biotechnology Co., Ltd.) was added to each well and incubated for 2 h. Absorbance was measured at 450 nm to assess cell viability.

Tumor cell sphere forming assay. Liver cancer cells were suspended in 200 μl of DMEM (Gibco; Thermo Fisher Scientific, Inc.) at a density of 1,000 cells per well, cultured in 96-well clear ultra-low attachment U-plates (Invitrogen; Thermo Fisher Scientific, Inc.) was incubated at 37˚C for 2 days. Culture medium was refreshed with a complete medium containing 5-FU (Huh7: 4.5 μM; Hep3B: 6.5 μM; JHH7: 2.0 μM; HepG2: 2.5 μM) or with hMAO-B-IN-9 (1.58 μM) (cat. no. HY-163879, MedChemExpress). The culture medium was replaced every 3 days, and the cells were continuously cultured in a cell incubator at 37˚C and 5% CO_2 for 13 days. The size of the spheroids derived from liver cancer cells were captured using an inverted microscope.

5-Ethynyl-2-deoxyuridine assay. To assess cell proliferation, the BeyoClick™ EdU-555 kit (cat. no. C0075S, Beyotime

Institute of Biotechnology) was used to evaluate DNA synthesis in liver cancer cells. The experiment was carried out according to the manufacturer's instructions. All experiments were carried out in triplicate, as described previously (34).

Levels of malondialdehyde (MDA) and glutathione (GSH) peroxidase (GPX) in liver cancer cells. Liver cancer cells were seeded in culture dishes and collected when the cell density reached 80%. Cells were lysed using Western and IP cell lysis buffer (cat. no. P0013; Beyotime Institute of Biotechnology), and then the supernatant was collected by centrifugation at 12,000 g at 4˚C for 10 min for subsequent assays. MDA content in the cells was measured using the Lipid Peroxidation (MDA) Assay Kit (cat. no. HY-K0319; MedChemExpress) according to the manufacturer's instructions. Absorbance was measured at 532 nm using a microplate reader, and the resulting values were compared with a standard curve to determine the concentration of MDA. GSH and GPX4) activity were also tested using Reduced Glutathione (GSH) Colorimetric Assay (cat. no. E-BC-K030-M) and Glutathione Peroxidase 4 (GPX4) Activity Assay Kit (E-BC-K883-M; both Elabscience Biotechnology Co., Ltd.) following the manufacturer's instructions.

Colony formation assay. Control Huh7 and Hep3B cells, and TTN-overexpressing Huh7 and Hep3B cells were seeded in 6-well plates at 500 cells per well and cultured for 2 weeks with replacement of the culture medium containing 5-FU (Huh7: 4.5 μM; Hep3B: 6.5 μM) every 3 days. After 2 weeks of incubation, cells were gently washed with PBS three times (3 min each), fixed with 4% paraformaldehyde for 30 min at room temperature, and washed three times with PBS for 3 min each. Cells were then stained with 1% crystal violet for 30 min at room temperature. After washing with PBS, the dishes were dried, and colonies with diameter >100 μm were counted. Clone count and size measurements were performed using ImageJ version 1.53t software (National Institutes of Health).

In vivo experiments. All animal experiments were conducted following the '3R' principles (replacement, reduction and refinement) and were approved by the Animal Care Committee of Guizhou Medical University under approval no. 2400641. A total of 10 female and 10 male (age, 4-6 weeks of 16-18 g BALB/c nude mice were purchased from Beijing Huafukang Biotechnology Co., Ltd., and after receiving the mice, they were acclimatized for 2 weeks in a specific pathogen-free environment at 25˚C and humidity of 30%. The mice were exposed to a 12-h light/dark cycle, and were given free access to mouse feed sterilized and water sterilized by autoclaving. For tumor growth experiments, BALB/c mice were randomly assigned to shNC and shTTN groups, 10 mice per group). HepG2/shNC or HepG2/shTTN cells ($6x10^5$ cells/100 μl) were resuspended in PBS containing 1% Matrigel and subcutaneously injected into the right abdomen of BALB/c mice. After 1 week, when tumors reached ~10 mm^3, the mice were randomly divided into two groups: One treated with Di-methyl sulfoxide (DMSO) control, and the other with 5-FU (25 mg/kg; 100 μl; intraperitoneal injections, once daily for 3 weeks). Tumor size was measured every 3 days, and tumor volume was calculated using the formula: Volume=1/2 (length x $width^2$). The mice were monitored for signs of poor health, including weight loss, postural abnormality, changes in activity levels, breathlessness, and signs of distress. Humane endpoints included maximum tumor volume >2,000 mm^3, ulceration, necrosis or infection on the surface of the tumor, weight loss >20%, abnormal posture, tumor affecting motor function, dyspnea, inability to eat and drink normally, the experiment was terminated, all mice were anesthetized with sodium pentobarbital at 5.0 mg/100 g body weight and sacrificed by cervical dislocation, and death was confirmed without breathing and heartbeat for more than 5 min. Tumors were harvested for weight measurement and histological analysis.

Immunohistochemical (IHC) staining. The tumor tissue was fixed in 4% paraformaldehyde at room temperature for 24 h, dehydrated in graded ethanol and embedded in paraffin, embedded in paraffin, and sectioned into 4 μm slices. After paraffin was removed with xylene at room temperature, and the tissue sections were gradually hydrated using ethanol. Antigen retrieval was performed using tris-EDTA antigen retrieval solution (pH 9.0; tris-EDTA antigen retrieval solution; Beyotime Institute of Biotechnology) at 95-100˚C for 15 min for antigen retrieval. To reduce non-specific binding, tissues were blocked with a solution containing 3% hydrogen peroxide for 10 min at room temperature, and 5% bovine serum albumin (Beijing Solarbio Science & Technology Co., Ltd.) for 1 h at room temperature. Tissues were incubated overnight at 4˚C with primary antibodies: Anti-Ki67 (1:400; cat. no. 2807-1-AP) and anti-PCNA (1:400; cat. no. 60097-1-IG) (both from Proteintech Group, Inc.). After washing with PBS, tissues were incubated with the secondary antibody (goat anti-rabbit/mouse HRP-labeled polymer; cat. no. PR30009 Proteintech Group, Inc.) for 2 h at 37˚C. The tissues were then stained with 3,3'-Diaminobenzidine tetrahydrochloride (Shanghai Yeasen Biotechnology Co., Ltd.) and counterstained with hematoxylin for 3 min at room temperature to visualize the cell nuclei. The antigen-antibody complex binding was detected using a light microscope.

Statistical analysis. Statistical analysis was carried out using Prism software (version 6.0; Dotmatics). Data are presented as the mean ± standard deviation. All experiments were conducted in triplicate. Statistical significance was determined using an unpaired Student's t-test or one-way ANOVA with Tukey's post hoc test. The Benjamini-Hochberg method was used to control the false discovery rates. $P<0.05$ was considered to indicate a statistically significant difference.

Results

Landscape of somatic variant and identification of molecular mechanisms affected by TTN mutations in liver cancer. Genome-wide mutation profiling in liver cancer was conducted by analyzing somatic mutation data, revealing that missense mutations were the most common variant types, followed by nonsense and frameshift deletion mutations, with single nucleotide polymorphisms (SNPs) accounting for the majority of variant types. The C>T transition emerged as the most prevalent single nucleotide variant (SNV; Fig. 1A). The number of mutant bases per patient was quantified, with a median

value of 1. TTN was identified as the gene with the highest mutation frequency in liver cancer. The top 10 most frequently mutated genes-TP53, TTN, CTNNB1, MUC16, ALB, PCLO, MUC4, RYR2, ABCA13 and APOB-demonstrated high mutation frequencies and distinct somatic mutation patterns (Fig. 1B). Analysis of tissue mutation characteristics in TCGA database revealed a positive correlation between TTN mutations and poor prognosis in liver cancer (HR=136.69; 95% CI=1.36-13,766.33; Fig. 1C). To elucidate the molecular mechanisms underlying TTN mutations in liver cancer, differential expression analysis was conducted on TTN-mutant and TTN-wild-type liver cancer tissues from TCGA database. The analysis revealed 140 downregulated genes and 30 upregulated genes (Fig. 1D and E). in TTN-mutant and -wild-type liver cancer (Fig. 1E). BP term enrichment analysis of the upregulated DEGs identified significant enrichment in terms such as 'Complement activation', 'positive regulation of cell activation', 'stress response to metal ions', 'glutathione metabolism' and 'cellular response to metal ions' (Fig. 1F). KEGG pathway analysis further indicated enrichment in pathways including 'mineral absorption', 'neuroactive ligand-receptor interaction', 'ferroptosis', 'fat digestion and absorption' and 'pancreatic secretion' (Fig. 1G). Notably, the BP terms impacted by TTN-mutant DEGs were associated with stress responses to metal ions and GSH metabolism. Additionally, KEGG pathway enrichment highlighted the association of these differential genes with ferroptosis. Given that numerous studies have established a connection between GSH metabolism and ferroptosis (35,36), these observations suggest that TTN mutations may influence liver cancer progression through the modulation of ferroptosis-related metabolic processes.

TTN mutations increase the sensitivity of liver cancer cells to GSK1904529A and nilotinib. To assess the impact of TTN mutations on drug sensitivity in liver cancer, the OncoPredict algorithm was used. A total of 198 drugs were analyzed, revealing significant changes in the drug scores of four drugs in liver cancer tissues with TTN mutations (Fig. 2A and B). Specifically, the drug scores for GSK1904529A and nilotinib were decreased in TTN-mutant liver cancer tissues, while 5-FU and sapitinib scores were increased (Fig. 2C and D). This suggests that TTN mutations may increase sensitivity to GSK1904529A and nilotinib while conferring resistance to 5-FU and sapitinib. To validate these observations, liver cancer cell lines with and without TTN mutations were analyzed using the CCLE database. Three TTN-mutant cell lines (Huh7, Hep3B and SNU182) and three wild-type cell lines (JHH7, HepG2 and LI7) were selected for further experiments. CCK-8 assays were carried out to determine IC_{50} values. For GSK1904529A, the IC_{50} values in 48 h were as follows: JHH7 (0.4156 μM), HepG2 (0.3501 μM), LI7 (0.2572 μM), Huh7 (0.0720 μM), Hep3B (0.0836 μM) and SNU182 (0.1107 μM). For nilotinib, IC_{50} values were: JHH7 (10.470 μM), HepG2 (6.200 μM), LI7 (5.049 μM), Huh7 (3.342 μM), Hep3B (3.675 μM) and SNU182 (2.010 μM). The IC_{50} values of 5-FU were as follows: JHH7 (2.251 μM), HepG2 (2.831 μM), LI7 (2.347 μM), Huh7 (4.618 μM), Hep3B (6.624 μM) and SNU182 (4.950 μM). Finally, for sapitinib, IC_{50} values were: JHH7 (2.140 nM), HepG2 (1.946 nM), LI7 (1.737 nM), Huh7 (7.749 nM), Hep3B (5.203 nM) and SNU182 (4.375 nM; Fig. 2E). Statistical analysis using the unpaired student's t-test indicated that the IC_{50} values for 5-FU and sapitinib were increased in TTN-mutant liver cancer cells, while the IC_{50}s for GSK1904529A and nilotinib were decreased when compared with their wild-type counterparts (Fig. 2F). These results suggest that TTN mutations may enhance sensitivity to GSK1904529A and nilotinib while contributing to resistance against 5-FU and sapitinib.

TTN mutations enhance the stability of the TTN protein. To validate the effect of TTN mutations on gene expression, the transcription levels of TTN were analyzed in liver cancer tissues from TCGA cohort. No significant difference was observed in the transcriptional levels of TTN between mutant and wild-type liver cancer tissues (Fig. 3A). Similarly, RT-qPCR experiments revealed no marked difference in TTN mRNA expression between TTN-mutant and wild-type liver cancer cell lines (Fig. 3B). However, despite similar mRNA levels, TTN protein expression was notably higher in TTN-mutant liver cancer cells (JHH7, HepG2 and Li7) (Fig. 3C). To explore the underlying mechanisms, protein synthesis was inhibited using cycloheximide (CHX; 1 μM), revealing that TTN protein stability was increased in TTN-mutant cells, with slower degradation when compared with wild-type cells (Fig. 3D). These results indicate that single nucleotide missense mutations in TTN enhance the stability of the encoded protein.

Increased TTN protein in liver cancer cells with TTN wild-type reduce the sensitivity to 5-FU. 5-FU, an uracil analog, is an effective anti-cancer drug. Previous studies have demonstrated its potent antitumor activity, both as a monotherapy and in combination with other chemotherapeutic agents, across a variety of different types of cancer, including lung cancer, hepatocellular carcinoma, colorectal cancer and gastric cancer (37-40). The present study further investigated the role of TTN protein in mediating 5-FU resistance in liver cancer cells. To enhance expression of TTN, plasmids were introduced into Huh7 and Hep3B cells (Fig. 4A). Studies have highlighted the role of metal ions in various physiological processes, including cellular homeostasis, metabolic regulation, biosynthesis, signal transduction and energy conversion (41,42), As studies examining the relationship between metal ions and cancer treatment progress, several metal ions have been found to induce apoptosis and enhance sensitivity to chemotherapeutic drugs (43,44). BP and KEGG pathway analyses revealed associations between TTN mutations and both metal ion metabolism and GSH metabolism (Fig. 1F), with ferroptosis pathway enrichment also observed (Fig. 1F). Building on these findings, the effects of TTN overexpression on the levels of ferrous and other metal ions in liver cancer cells were explored. The results revealed that TTN overexpression or 5-FU treatment had minimal impact on the levels of zinc, calcium and copper ions in the cells (Fig. 4B). Notably, TTN overexpression significantly inhibited the increase in ferrous ion levels in 5-FU-treated Huh7 and Hep3B cells compared with 5-FU-treated negative control (Fig. 4C). Further analysis of ferroptosis-related markers revealed that TTN overexpression reduced MDA content in 5-FU-treated cells and increased levels of GSH and GPX4 compared with the 5-FU-treated negative control group, effectively reversing

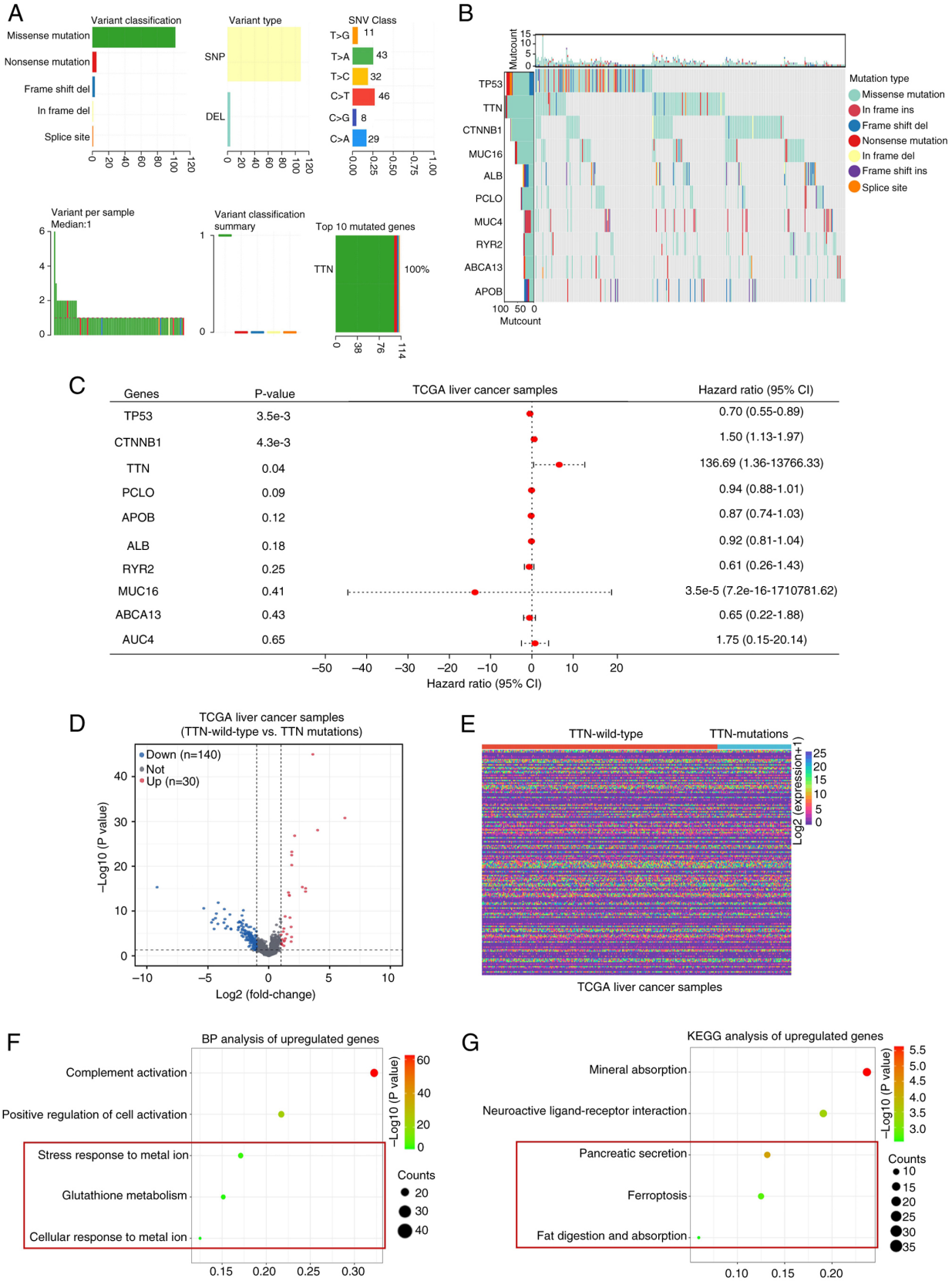

Figure 1. Comprehensive profiling of somatic mutation data and DEGs between samples of liver cancer with either mutated or wild-type TTN, with enrichment analysis. (A) Variant classification in liver cancer, highlighting missense mutations as the most frequent, with SNPs comprising the majority of variant types. C > T is the most common type of SNV. The number of mutated bases per patient is displayed, with a median of 1. The top mutated gene, TTN, is indicated. (B) Waterfall plot illustrating the distribution of variant classifications across all patients with liver cancer. (C) Overall survival analysis of patients with liver cancer carried out using the Cox proportional hazards model. (D) Volcano plot depicting gene expression changes between TCGA liver cancer datasets harboring either TTN mutations or wild-type TTN. (E) Heatmap displaying the DEGs between TCGA liver cancer datasets harboring either TTN mutations or wild-type TTN. (F) BP analysis and (G) KEGG pathway enrichment analysis of the 30 upregulated genes common to both conditions. DEL, Deletion; SNP, single nucleotide polymorphism; SNV, single nucleotide variation; TTN, titin; TCGA, The Cancer Genome Atlas; CI, confidence interval; BP, biological processes; KEGG; Kyoto Encyclopedia of Genes and Genomes; DEGs, differentially expressed genes; Mut, mutation.

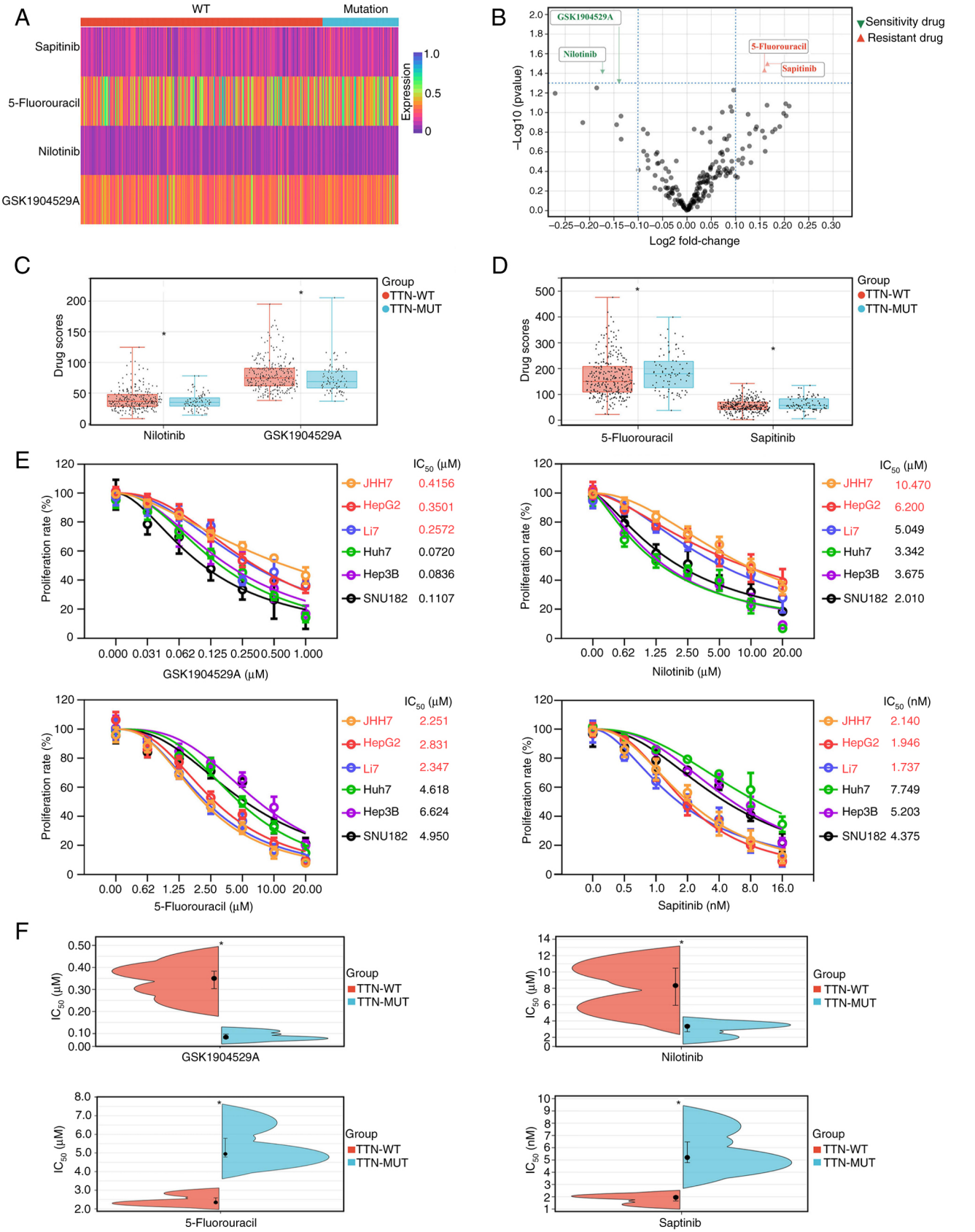

Figure 2. TTN mutations increase liver cancer cell sensitivity to GSK1904529A and nilotinib. (A) Heatmap showing the differential drug sensitivity in liver cancer cells with TTN mutation vs. TTN wild-type. (B) OncoPredict algorithm analysis of drug response scores for 198 drugs in liver cancer tissues with TTN mutations compared with TTN wild-type. (C) Drug response scores for GSK1904529A and nilotinib in liver cancer tissues with mutated and wild-type TTN. (D) Drug response scores for fluorouracil and sapitinib in liver cancer tissues with either mutated or wild-type TTN. Huh7, Hep3B and SNU182 harbor TTN mutations, while JHH7, HepG2 and Li7 are TTN wild-type. (E) CCK-8 assays used to assess the IC_{50} of GSK1904529A, nilotinib, fluorouracil and sapitinib in JHH7, HepG2, Li7, Huh7, Hep3B and SNU182 liver cancer cell lines over 48 h. (F) Comparison of IC_{50} values for GSK1904529A, nilotinib, fluorouracil and sapitinib between liver cancer cells with mutated or wild-type TTN. $^{*}P<0.05$, n=3. The control group was used for comparison. Data are presented as mean ± SD. TTN, titin; TTN-WT, wild-type titin; TTN-MUT, mutated titin; CCK-8, Cell Counting Kit-8.

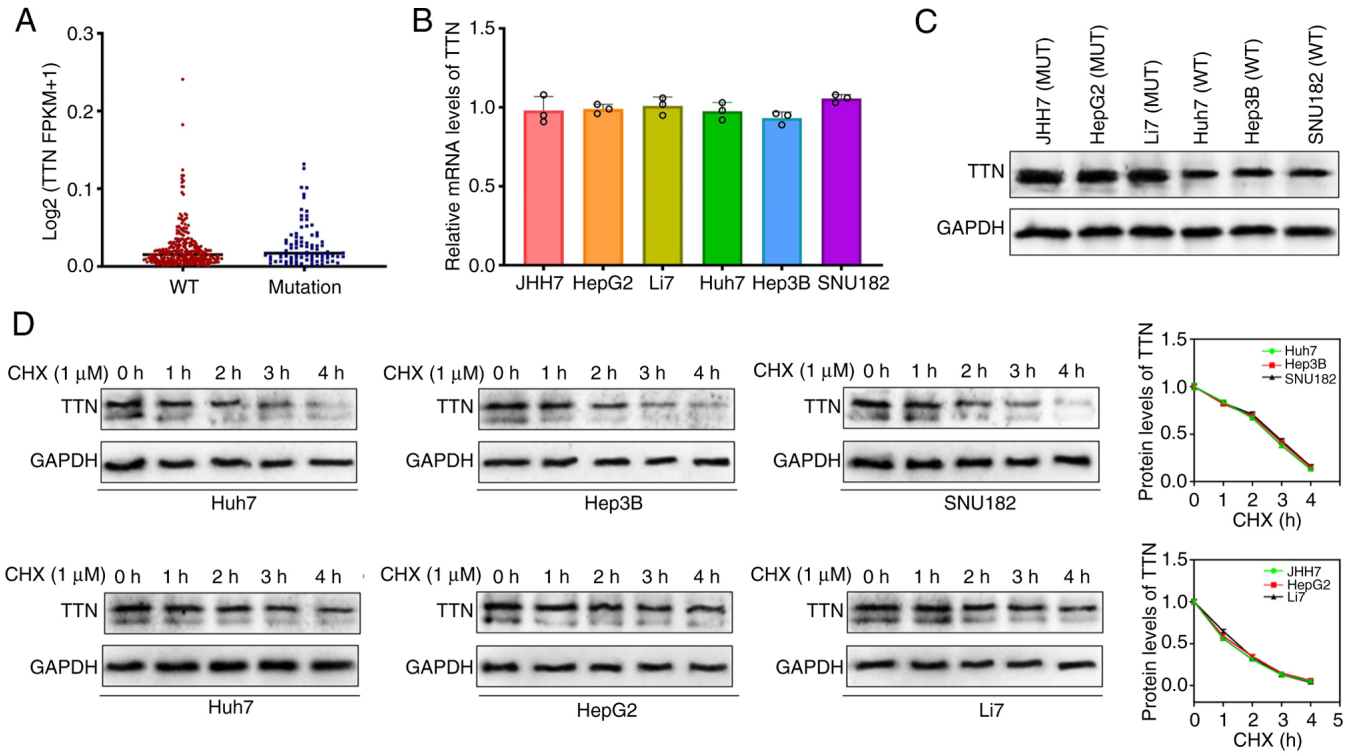

Figure 3. TTN mutation enhances the stability of the TTN protein. (A) TTN mRNA expression levels in liver cancer tissues with mutated TTN (blue dots) and wild-type TTN (red dots) from TCGA databases. A total of 86 patients with liver cancer with TTN-MUT and 274 with TTN-WT were included. (B) TTN mRNA expression levels in liver cancer cell lines: JHH7, HepG2, Li7, Huh7, Hep3B and SNU182. (C) TTN protein expression levels in JHH7, HepG2, Li7, Huh7, Hep3B and SNU182 cell lines (D) TTN protein degradation rate in JHH7, HepG2, Li7, Huh7, Hep3B and SNU182 cells (uncropped images available in the Supplementary file). Data are presented as mean ± SD. TTN, titin; TTN-WT, wild-type titin; TTN-MUT, mutated titin; TCGA, The Cancer Genome Atlas.

5-FU-induced ferroptosis (Fig. 4D). Additionally, while TTN overexpression did not significantly impact colony formation, tumor spheroid formation or DNA synthesis rates, it notably mitigated the inhibitory effects of 5-FU on these processes (Fig. 4E-G). These results suggest that increased TTN expression levels may inhibit ferroptosis in tumor cells, thereby enhancing liver cancer resistance to 5-FU.

TTN knockdown enhances sensitivity to 5-FU in liver cancer cells with TTN mutations. TTN protein function in liver cancer cells harboring TTN mutations was further investigated. Three specific shRNAs were employed to knockdown TTN expression in JHH7 and HepG2 cells (Fig. 5A and B). TTN knockdown did not significantly affect the cellular levels of zinc, calcium, copper or ferrous ions. However, following 5-FU treatment, ferrous ion levels in the sh2 and sh3 groups increased significantly compared with shNC group (Fig. 5C and D). Additionally, MDA levels were significantly higher in the sh2 and sh3 groups following 5-FU treatment compared with shNC, while GPX4 and GSH levels were significantly decreased (Fig. 5E).

Knockdown of TTN enhances the suppressive effects of 5-FU on cell proliferation. TTN knockdown in JHH7 and HepG2 cells also enhanced the inhibitory effect of 5-FU on DNA synthesis rates (Fig. 6A), and tumor spheroid proliferation (Fig. B). Treatment with the ferrous ion chelator hMAO-B-IN-9 slightly reversed these inhibitory effects (Fig. 6A and B).

Knockdown of TTN enhances the therapeutic effect of 5-FU in vivo. *In vivo*, the synergistic effect of TTN deletion with 5-FU was explored by transplanting HepG2/shNC or HepG2/shTTN cells into the subcutaneous tissue of immunocompromised BABL/c mice. Tumor-bearing mice were treated with DMSO or 5-FU (25 mg/kg; 100 μl) via intraperitoneal injection once daily for 21 days (Fig. 7A). TTN knockdown did not significantly impact tumor growth in HepG2/shNC cells (Fig. 7B-D). However, stable TTN knockdown increased the sensitivity of tumors to 5-FU, significantly inhibiting tumor growth in mice transplanted with HepG2/shTTN cells (Fig. 7B-D). IHC staining of tumor tissue revealed that, similar to the *in vitro* results, the levels of Ki67 and PCNA were significantly lower in TTN-knockdown tumors compared with the control following 5-FU treatment (Fig. 7E-G). These results underscore the potential role of TTN mutations in modulating 5-FU sensitivity in liver cancer.

Discussion

Liver cancer continues to be a major global health issue, characterized by rising morbidity and mortality; there were ~865,000 new cases and 757,948 deaths worldwide in 2022 (45). The onset and progression of liver cancer exhibits considerable molecular heterogeneity, with complex underlying mechanisms involving various genetic abnormalities, such as SNPs, genomic instability, somatic mutations and dysregulated signaling pathways (46,47). Genomic instability is a hallmark of liver cancer, and an accumulation of gene

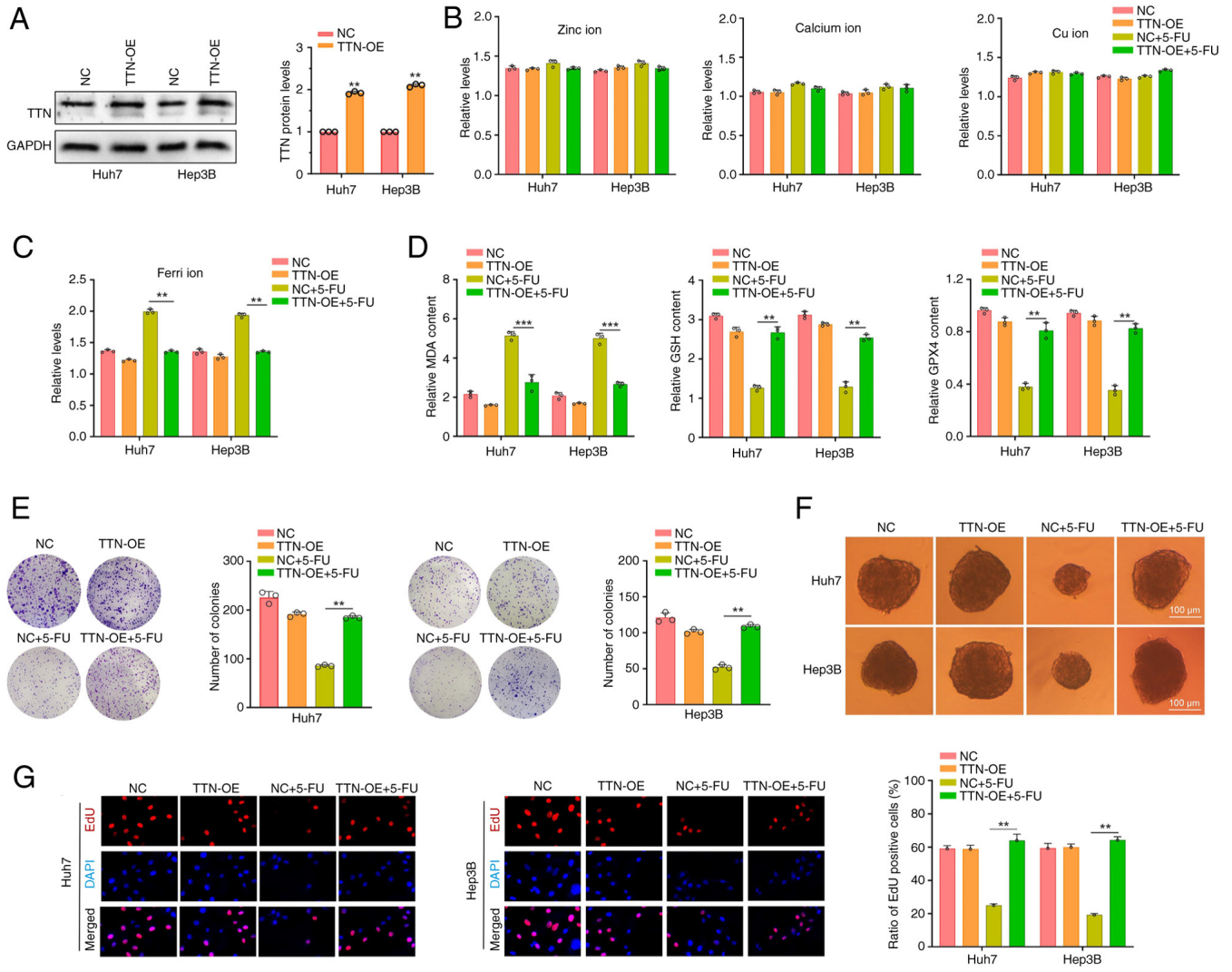

Figure 4. Overexpression of TTN protein in liver cancer cells with wild-type TTN reduces sensitivity to 5-FU. (A) TTN plasmid transfection into Huh7 and Hep3B cells to establish TTN overexpression models. NC group: Cells transfected with an empty vector pCDNA3.1 without the target gene. (B) Spectrophotometric analysis of zinc, calcium, cu, and (C) ferri ion levels in Huh7 and Hep3B cells following TTN overexpression and 5-FU treatment. (D) MDA, GSH and GPX4 content in Huh7 and Hep3B cells after TTN overexpression and 5-FU treatment. (E) Colony formation assay in Huh7 and Hep3B cells following TTN overexpression and 5-FU treatment. (F) Tumor sphere formation assay in Huh7 and Hep3B cells after TTN overexpression and 5-FU treatment. (G) EdU staining of Huh7 and Hep3B cells following TTN overexpression and 5-FU treatment. **P<0.01, ***P<0.001, n=3. Data are presented as mean ± SD. TTN, titin; 5-FU, 5-fluorouracil; NC, negative control; TTN-OE, titin overexpression; Cu, copper; Ferri, ferrous ions; MDA, malondialdehyde; GSH, glutathione; GPX4, glutathione peroxidase 4.

mutations is associated with tumorigenesis. These mutations contribute to the acquisition of cancer cell traits, including uncontrolled proliferation, immune evasion, invasion, metastasis and resistance to therapies (18,48). The advent of high-throughput sequencing technologies has enhanced understanding of the pathological processes underlying liver cancer and facilitated the identification of key genes involved in its carcinogenesis (18,49). However, the precise biological effects and molecular mechanisms associated with liver cancer gene mutations remain poorly understood.

The present study demonstrates that TTN mutations are prevalent in liver cancer, as evidenced by the analysis of somatic mutation data from liver cancer tissues in TCGA cohort. These mutations associate with prognosis and resistance to treatment in liver cancer. Differential gene expression analysis and enrichment analysis revealed that TTN mutations significantly influence metal ion metabolism, GSH metabolism and ferroptosis. High frequencies of TTN mutations have also been identified in several other types of cancer, including non-small cell lung cancer, ovarian cancer, breast cancer, small cell lung cancer and colon adenocarcinoma (24,50). Findings of the present study revealed an association between TTN mutations and dysregulated iron ion metabolism and GSH metabolism, along with enrichment in the ferroptosis pathway.

Ferroptosis, an iron-dependent form of cell death distinct from autophagy, apoptosis and necrosis (51), has a pivotal role in inhibiting tumorigenesis and offers new therapeutic avenues for the treatment of cancer (52). TTN mutations may indirectly affect the occurrence of ferroptosis by affecting various mechanisms such as cytoskeletal stability, calcium homeostasis, mitochondrial function, iron metabolism and gene expression (53-56). The present study revealed that the increase in protein stability after TTN mutation in liver cancer mainly affected the expression of GPX4 and GSH, key

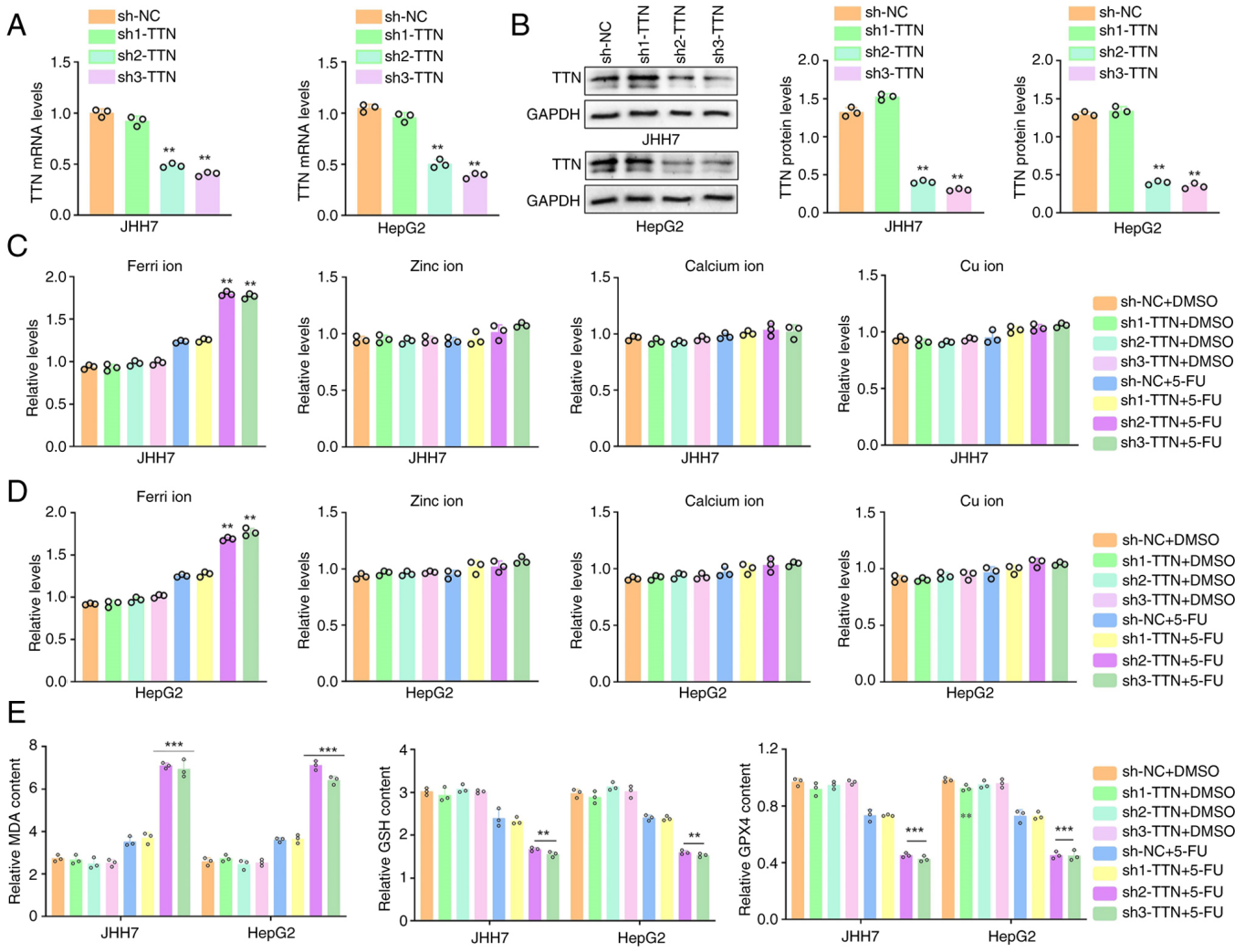

Figure 5. TTN knockdown enhances sensitivity to 5-FU in liver cancer cells with mutated TTN. TTN shRNAs were transfected into JHH7 and HepG2 cells to generate TTN knockdown models (uncropped images available in the Supplementary file). Efficiency of shRNAs was assessed by (A) RT-qPCR and (B) western blotting. Spectrophotometric analysis of zinc ion, calcium ion, cu ion and ferri ion levels in (C) JHH7 and (D) HepG2 cells following TTN knockdown and 5-FU treatment. (E) Measurement of MDA, GSH and GPX4 levels in JHH7 and HepG2 cells after TTN knockdown and 5-FU treatment. **P<0.01, ***P<0.001, n=3. Data are presented as mean ± SD. TTN, titin; FU, 5-fluorouracil; NC, negative control; malondialdehyde, MDA; GSH, glutathione; GPX4, glutathione peroxidase 4.

regulators of ferroptosis, and reduced intracellular iron ion concentration, thereby inhibiting ferroptosis. However, the relationship between TTN mutation and ferroptosis has not been fully elucidated, and future work explore the association between TTN mutations and ferroptosis.

Despite advances in liver cancer treatment, drug resistance remains a major clinical challenge. Several chemotherapy agents have been found to induce ferroptosis, and resistance to treatment is associated with the dysregulation of this process (57). Studies indicate that cancer cells become resistant through GPX4-mediated regulation of lipid peroxidation, further implicating ferroptosis in treatment failure (58-60). Building on these findings, the present study suggests that TTN mutations may enhance liver cancer resistance by inhibiting the ferroptosis pathway. Moreover, OncoPredict analysis and CCK-8 assays revealed that TTN mutations increased sensitivity to GSK1904529A and nilotinib, while conferring resistance to 5-FU and saptinib in liver cancer cells. However, there are limitations to the association between drug susceptibility scores and clinical outcomes. At present, the evaluation method of the drug susceptibility score is not fully standardized, and different detection techniques and scoring systems may produce different results. In addition, factors such as tumor heterogeneity, individual differences in patients, and other factors can also affect the correlation between drug sensitivity scores and clinical outcomes.

Predictions made by OncoPredict are based on network databases and do not fully capture the molecular changes in individual patients, highlighting the need for additional *in vitro* cell line testing and patient-derived xenograft models. Since its discovery, 5-FU has remained a cornerstone in the treatment of solid tumors, including liver cancer (61). Upon entering the cell, 5-FU is metabolized into several active metabolites, such as fluorodeoxyuridine triphosphate and fluorodeoxyuridine monophosphate, which inhibit thymidylate synthetase and exert cytotoxic effects (62). Results of the present study indicate that TTN mutations stabilize

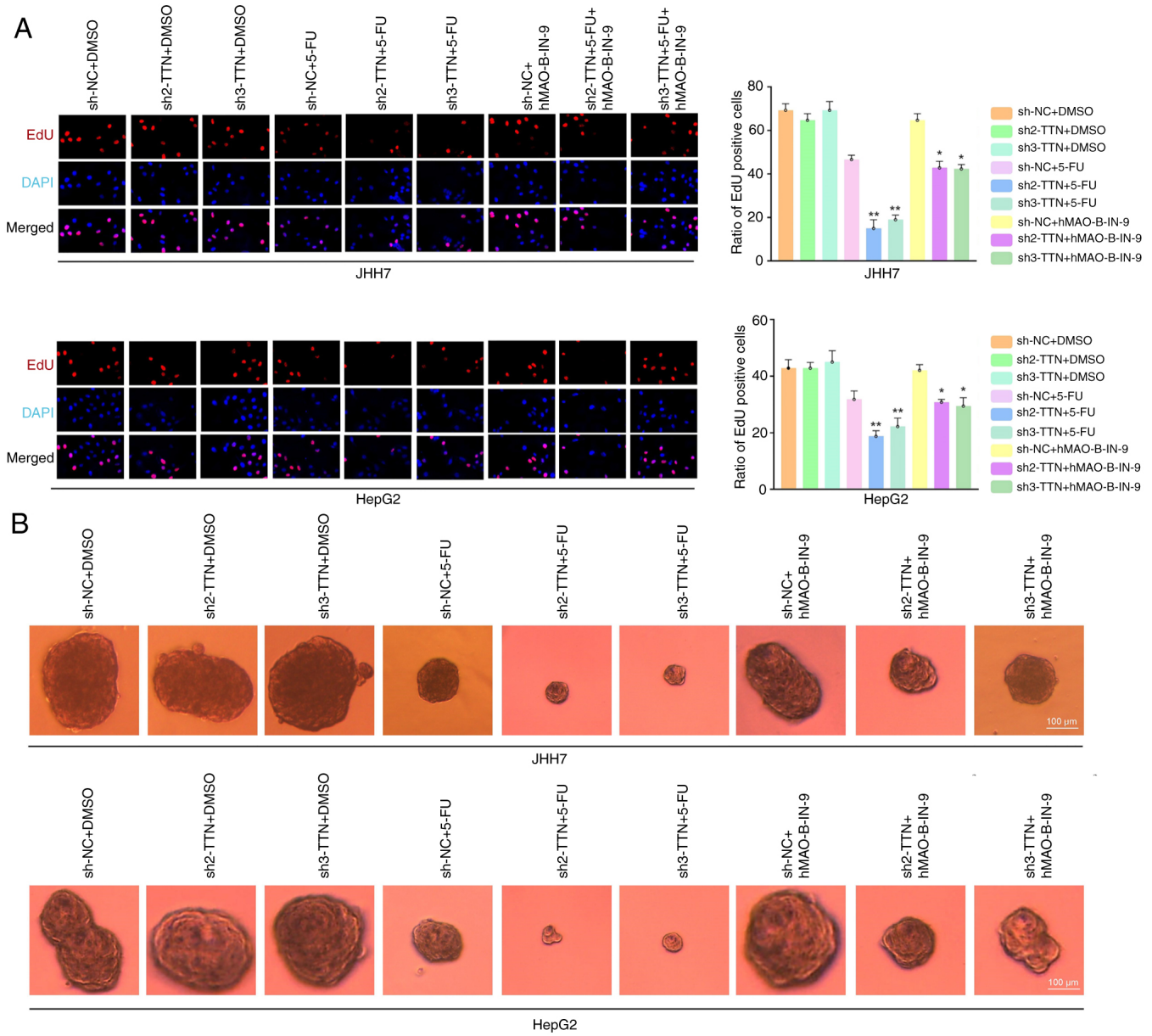

Figure 6. Knockdown of TTN enhances the suppressive effects of 5-FU on cell proliferation. (A) EdU staining of JHH7 and HepG2 cells after TTN knockdown and 5-FU treatment, with or without hMAO-B-IN-9 treatment. (B) Tumor sphere formation assay in JHH7 and HepG2 cells following TTN knockdown and 5-FU treatment, with or without hMAO-B-IN-9 treatment. *P<0.05, **P<0.01, n=3. Data are presented as mean ± SD. TTN, titin; 5-FU, 5-fluorouracil; NC, negative control.

TTN protein, suppress ferroptosis by reducing intracellular iron ion levels and significantly diminish the sensitivity of liver cancer cells to 5-FU both *in vitro* and *in vivo*. The present study provides preliminary evidence suggesting that TTN mutations may serve as a prognostic biomarker for liver cancer and contribute to treatment resistance. The specific effects of TTN gene mutations vary depending on factors such as the type of mutation, the location of the mutation and the genetic background of the individual. For example, missense mutations cause one amino acid to be replaced with another, altering the function of a protein. A nonsense mutation produces a stop codon that results in an early termination of protein synthesis. Deletion mutations and insertional mutations may introduce alterations in the reading frame, resulting in severe alterations or deletions of protein sequences, resulting in loss of function (63). At present, there is still insufficient research on the effects of different types of TTN mutations on liver cancer, warranting further exploration of the biological or therapeutic implications of the different types of TTN mutations in liver cancer in future studies.

The present study has limitations, particularly the absence of clinical validation and the reliance on animal and cellular models for experimental evidence. Future studies should focus on clinical trials and xenotransplantation models derived from patient samples to validate the *in vitro* and *in vivo* findings of the present study and strengthen the clinical relevance of these observations.

In conclusion, TTN mutations represent a high-frequency genetic alteration in liver cancer, enhancing TTN protein

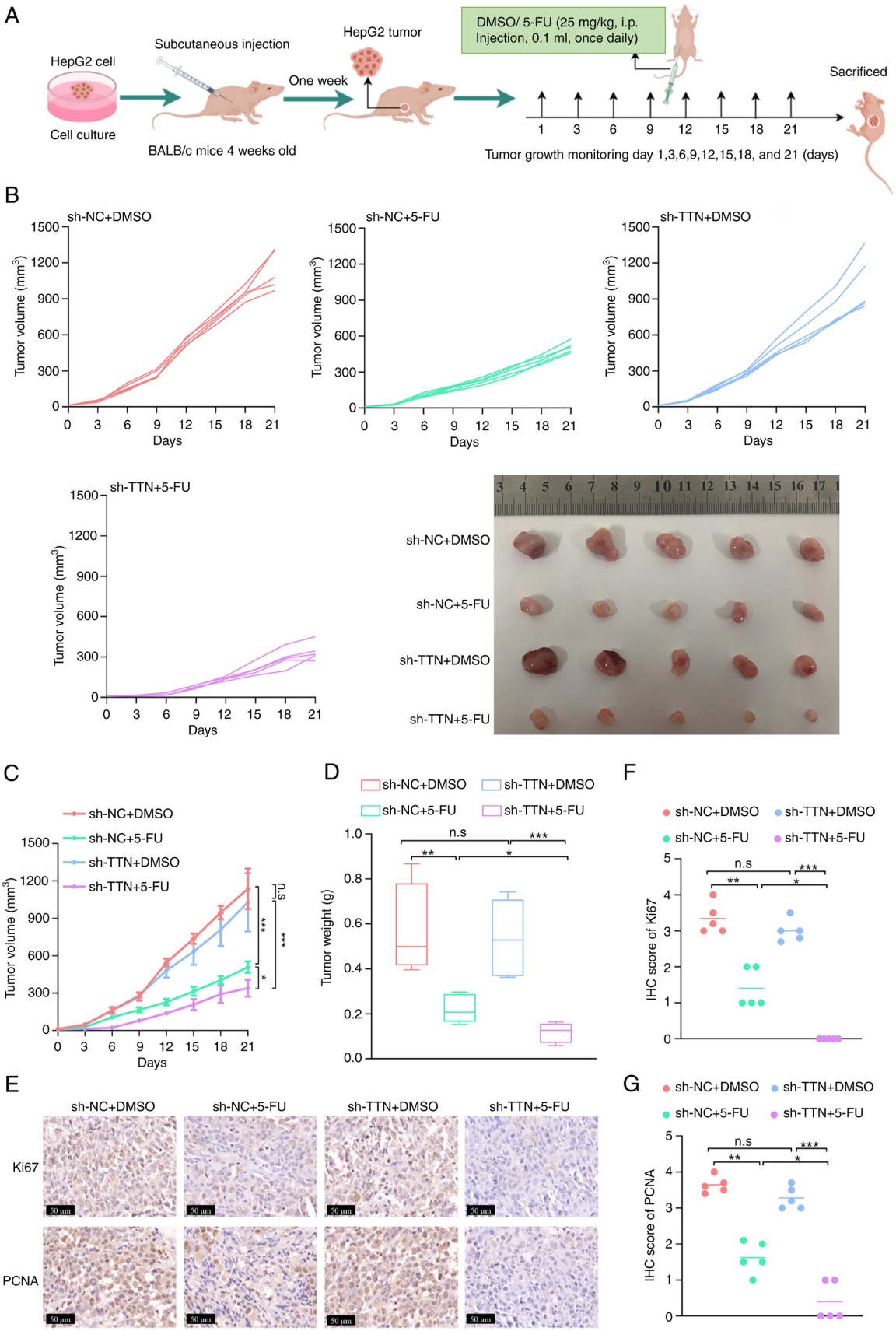

Figure 7. Knockdown of TTN enhances the therapeutic effect of 5-FU *in vivo*. (A) Tumor growth of HepG2/shNC and HepG2/shTTN cells in subcutaneous xenografts of immunocompromised BABL/c mice. Tumor-bearing mice were treated with intraperitoneal injections of DMSO (control) or 5-FU (25 mg/kg; 100 μl) once daily for 21 days. (B) Tumor growth curves (n=5). Tumors were harvested after 21 days of DMSO or 5-FU treatment (n=5). (C) Tumor volume and (D) weight (n=5). (E) Representative immunohistochemistry images showing Ki67 and PCNA expression in tumor tissues (magnification, 400x; scale bars, 50 μm; n=5). Quantification of (F) Ki67 and (G) PCNA expression levels in tumor tissues using ImageJ software. All results are shown as mean ± SD. *P<0.05, **P<0.01, ***P<0.001, n=3. Data are presented as mean ± SD. TTN, titin; 5-FU, 5-fluorouracil; NC, negative control; i.p., intraperitoneal; IHC, immunohistochemistry; n.s. not significant.

stability. Depletion of TTN leads to reduced intracellular iron ion levels, inhibiting ferroptosis and significantly decreasing liver cancer sensitivity to 5-FU both *in vitro* and *in vivo*. These findings highlight the potential role of TTN mutations in diminishing the effectiveness of 5-FU in liver cancer treatment. The present study is limited by the lack of clinical validation and is based solely on animal and cellular models. Further research is needed to confirm the therapeutic potential of targeting TTN mutations in overcoming liver cancer drug resistance.

Acknowledgements

Not applicable.

Funding

This research was funded by the National Natural Science Foundation of China (grant no. 82103681), the Guizhou Medical University National Natural Science Foundation Cultivation Project (grant nos. 20NSP020 and 19NSP034), the Guizhou Provincial Science and Technology Projects [grant no. ZK (2024)159], the Guizhou Provincial Science and Technology Projects [grant no. ZK (2024)169] and the Continuous Support Fund for Excellent Scientific Research Platforms of Colleges and Universities in Guizhou Province [grant no. QJJ (2022)020].

Availability of data and materials

The data generated in the present study may be requested from the corresponding author.

Authors' contributions

SL and TC contributed to conceptualization; SL stored and backed-up all data in the article; ZZh, YS and ZZe analyzed data. DL and WC performed bioinformatics analysis; ZZh and YS contributed to the methodology; SL contributed to the resources; SL and TC contributed to the software; SL and TC contributed to validation; ZZh contributed to writing the original draft; SL contributed to writing, reviewing and editing. ZZh and SL confirm the authenticity of all the raw data. All authors read and approved the final manuscript.

Ethics approval and consent to participate

The animal experiments were approved by the Animal Ethics Committee of Guizhou Medical University (approval no. 2400641). Tissue sample data used in the present study were sourced from public databases, such as TCGA and did not involve human ethics.

Patient consent for publication

Not applicable.

Competing interests

The authors declare that they have no competing interests.

References

1. Anwanwan D, Singh SK, Singh S, Saikam V and Singh R: Challenges in liver cancer and possible treatment approaches. Biochim Biophys Acta Rev Cancer 1873: 188314, 2020.
2. Singh SP, Arora V, Madke T and Sarin SK: Hepatocellular carcinoma-southeast asia updates. Cancer J 29: 259-265, 2013.
3. Mazzaferro V, Citterio D, Bhoori S, Bongini M, Miceli R, De Carlis L, Colledan M, Salizzoni M, Romagnoli R, Antonelli B, *et al*: Liver transplantation in hepatocellular carcinoma after tumour downstaging (XXL): A randomised, controlled, phase 2b/3 trial. Lancet Oncol 21: 947-956, 2020.
4. Reig M, Forner A, Rimola J, Ferrer-Fàbrega J, Burrel M, Garcia-Criado Á, Kelley RK, Galle PR, Mazzaferro V, Salem R, *et al*: BCLC strategy for prognosis prediction and treatment recommendation: The 2022 update. J Hepatol 76: 681-693, 2022.
5. Wong TC, Lee VH, Law AL, Pang HH, Lam KO, Lau V, Cui TY, Fong AS, Lee SW, Wong EC, *et al*: Prospective study of stereotactic body radiation therapy for hepatocellular carcinoma on waitlist for liver transplant. Hepatology 74: 2580-2594, 2021.
6. Tang W, Chen Z, Zhang W, Cheng Y, Zhang B, Wu F, Wang Q, Wang S, Rong D, Reiter FP, *et al*: The mechanisms of sorafenib resistance in hepatocellular carcinoma: Theoretical basis and therapeutic aspects. Signal Transduct Target Ther 5: 87, 2020.
7. Su X, Li Y, Ren Y, Cao M, Yang G, Luo J, Hu Z, Deng H, Deng M, Liu B and Yao Z: A new strategy for overcoming drug resistance in liver cancer: Epigenetic regulation. Biomed Pharmacother 176: 116902, 2024.
8. Kudo M, Finn RS, Qin S, Han KH, Ikeda K, Piscaglia F, Baron A, Park JW, Han G, Jassem J, *et al*: Lenvatinib versus sorafenib in first-line treatment of patients with unresectable hepatocellular carcinoma: A randomised phase 3 non-inferiority trial. Lancet 391: 1163-1173, 2018.
9. Finn RS, Qin S, Ikeda M, Galle PR, Ducreux M, Kim TY, Kudo M, Breder V, Merle P, Kaseb AO, *et al*: Atezolizumab plus bevacizumab in unresectable hepatocellular carcinoma. N Engl J Med 382: 1894-1905, 2020.
10. Wang Z, Wang Y, Gao P and Ding J: Immune checkpoint inhibitor resistance in hepatocellular carcinoma. Cancer Lett 555: 216038, 2023.
11. Ostroverkhova D, Przytycka TM and Panchenko AR: Cancer driver mutations: Predictions and reality. Trends Mol Med 29: 554-566, 2023.
12. Pirozzi CJ and Yan H: The implications of IDH mutations for cancer development and therapy. Nat Rev Clin Oncol 18: 645-661, 2021.
13. Shahbandi A, Nguyen HD and Jackson JG: TP53 mutations and outcomes in breast cancer: Reading beyond the headlines. Trends Cancer 6: 98-110, 2020.
14. Prior IA, Hood FE and Hartley JL: The frequency of ras mutations in cancer. Cancer Res 80: 2969-2974, 2020.
15. Timar J and Kashofer K: Molecular epidemiology and diagnostics of KRAS mutations in human cancer. Cancer Metastasis Rev 39: 1029-1038, 2020.
16. Herzog SK and Fuqua SAW: ESR1 mutations and therapeutic resistance in metastatic breast cancer: Progress and remaining challenges. Br J Cancer 126: 174-186, 2022.
17. Calderaro J, Couchy G, Imbeaud S, Amaddeo G, Letouzé E, Blanc JF, Laurent C, Hajji Y, Azoulay D, Bioulac-Sage P, *et al*: Histological subtypes of hepatocellular carcinoma are related to gene mutations and molecular tumour classification. J Hepatol 67: 727-738, 2017.
18. Wang P, Song Q, Ren J, Zhang W, Wang Y, Zhou L, Wang D, Chen K, Jiang L, Zhang B, *et al*: Simultaneous analysis of mutations and methylations in circulating cell-free DNA for hepatocellular carcinoma detection. Sci Transl Med 14: eabp8704, 2022.
19. Calderaro J, Ziol M, Paradis V and Zucman-Rossi J: Molecular and histological correlations in liver cancer. J Hepatol 71: 616-630, 2019.
20. Loescher CM, Hobbach AJ and Linke WA: Titin (TTN): From molecule to modifications, mechanics, and medical significance. Cardiovasc Res 118: 2903-2918, 2022.
21. Ceyhan-Birsoy O, Agrawal PB, Hidalgo C, Schmitz-Abe K, DeChene ET, Swanson LC, Soemedi R, Vasli N, Iannaccone ST, Shieh PB, *et al*: Recessive truncating titin gene, TTN, mutations presenting as centronuclear myopathy. Neurology 81: 1205-1214, 2013.

22. Kellermayer D, Smith JE III and Granzier H: Titin mutations and muscle disease. Pflugers Arch 471: 673-682, 2019.
23. Djulbegovic MB, Uversky VN, Karp CL and Harbour JW: Functional impact of titin (TTN) mutations in ocular surface squamous neoplasia. Int J Biol Macromol 195: 93-101, 2022.
24. Gomes FC, Figueiredo ERL, Araújo EN, Andrade EM, Carneiro CDL, Almeida GM, Dias HAAL, Teixeira LIB, Almeida MT, Farias MF, *et al*: Social, genetics and histopathological factors related to titin (TTN) gene mutation and survival in women with ovarian serous cystadenocarcinoma: Bioinformatics analysis. Genes (Basel) 14: 1092, 2023.
25. Han X, Chen J, Wang J, Xu J and Liu Y: TTN mutations predict a poor prognosis in patients with thyroid cancer. Biosci Rep 42: BSR20221168, 2022.
26. Kodali N, Alomary S, Bhattaru A, Eldaboush A, Schwartz RA and Lipner SR: Gender and melanoma subtype-based prognostic implications of MUC16 and TTN co-occurrent mutations in melanoma: A retrospective multi-study analysis. Cancer Med 13: e70199, 2024.
27. Xue D, Lin H, Lin L, Wei Q, Yang S and Chen X: TTN/TP53 mutation might act as the predictor for chemotherapy response in lung adenocarcinoma and lung squamous carcinoma patients. Transl Cancer Res 10: 1284-1294, 2021.
28. Liu Z, Zhao X, Wang R, Tang X, Zhao Y, Zhong G, Peng X and Zhang C: Heterogeneous pattern of gene expression driven by TTN mutation is involved in the construction of a prognosis model of lung squamous cell carcinoma. Front Oncol 13: 916568, 2023.
29. Chen R, Yao Z and Jiang L: Construction and validation of a TTN mutation associated immune prognostic model for evaluating immune microenvironment and outcomes of gastric cancer: An observational study. Medicine (Baltimore) 103: e38979, 2024.
30. Mayakonda A, Lin DC, Assenov Y, Plass C and Koeffler HP: Maftools: Efficient and comprehensive analysis of somatic variants in cancer. Genome Res 28: 1747-1756, 2018.
31. Robinson MD, McCarthy DJ and Smyth GK: edgeR: A bioconductor package for differential expression analysis of digital gene expression data. Bioinformatics 26: 139-140, 2010.
32. Maeser D, Gruener RF and Huang RS: oncoPredict: An R package for predicting in vivo or cancer patient drug response and biomarkers from cell line screening data. Brief Bioinform 22: bbab260, 2021.
33. Ruiz-Villalba A, Ruijter JM and van den Hoff MJB: Use and misuse of C_q in qPCR data analysis and reporting. Life (Basel) 11: 496, 2021.
34. Lei S, Cao W, Zeng Z, Zhang Z, Jin B, Tian Q, Wu Y, Zhang T, Li D, Hu C, *et al*: JUND/linc00976 promotes cholangiocarcinoma progression and metastasis, inhibits ferroptosis by regulating the miR-3202/GPX4 axis. Cell Death Dis 13: 967, 2022.
35. Chen X, Li J, Kang R, Klionsky DJ and Tang D: Ferroptosis: Machinery and regulation. Autophagy 17: 2054-2081, 2021.
36. Liang D, Feng Y, Zandkarimi F, Wang H, Zhang Z, Kim J, Cai Y, Gu W, Stockwell BR and Jiang X: Ferroptosis surveillance independent of GPX4 and differentially regulated by sex hormones. Cell 186: 2748-2764.e22, 2023.
37. Propper DJ, Gao F, Saunders MP, Sarker D, Hartley JA, Spanswick VJ, Lowe HL, Hackett LD, Ng TT, Barber PR, *et al*: PANTHER: AZD8931, inhibitor of EGFR, ERBB2 and ERBB3 signalling, combined with FOLFIRI: A phase I/II study to determine the importance of schedule and activity in colorectal cancer. Br J Cancer 128: 245-254, 2023.
38. Pereira M and Vale N: Repurposing alone and in combination of the antiviral saquinavir with 5-fluorouracil in prostate and lung cancer cells. Int J Mol Sci 23: 12240, 2022.
39. Guo J, Yu Z, Sun D, Zou Y, Liu Y and Huang L: Two nanoformulations induce reactive oxygen species and immunogenetic cell death for synergistic chemo-immunotherapy eradicating colorectal cancer and hepatocellular carcinoma. Mol Cancer 20: 10, 2021.
40. Yuan J, Khan SU, Yan J, Lu J, Yang C and Tong Q: Baicalin enhances the efficacy of 5-fluorouracil in gastric cancer by promoting ROS-mediated ferroptosis. Biomed Pharmacother 164: 114986, 2023.
41. Lin J, Bjørk PK, Kolte MV, Poulsen E, Dedic E, Drace T, Andersen SU, Nadzieja M, Liu H, Castillo-Michel H, *et al*: Zinc mediates control of nitrogen fixation via transcription factor filamentation. Nature 631: 164-169, 2024.
42. Jomova K, Makova M, Alomar SY, Alwasel SH, Nepovimova E, Kuca K, Rhodes CJ and Valko M: Essential metals in health and disease. Chem Biol Interact 367: 110173, 2022.
43. Luan M, Feng Z, Zhu W, Xing Y, Ma X, Zhu J, Wang Y and Jia Y: Mechanism of metal ion-induced cell death in gastrointestinal cancer. Biomed Pharmacother 174: 116574, 2024.
44. Sun X, Zhang Y, Li J, Park KS, Han K, Zhou X, Xu Y, Nam J, Xu J, Shi X, *et al*: Amplifying STING activation by cyclic dinucleotide-manganese particles for local and systemic cancer metalloimmunotherapy. Nat Nanotechnol 16: 1260-1270, 2021.
45. Bray F, Laversanne M, Sung H, Ferlay J, Siegel RL, Soerjomataram I and Jemal A: Global cancer statistics 2022: GLOBOCAN estimates of incidence and mortality worldwide for 36 cancers in 185 countries. CA Cancer J Clin 74: 229-263, 2024.
46. Forner A, Reig M and Bruix J: Hepatocellular carcinoma. Lancet 391: 1301-1314, 2018.
47. Vogel A, Meyer T, Sapisochin G, Salem R and Saborowski A: Hepatocellular carcinoma. Lancet 400: 1345-1362, 2022.
48. Sun Y, Wu P, Zhang Z, Wang Z, Zhou K, Song M, Ji Y, Zang F, Lou L, Rao K, *et al*: Integrated multi-omics profiling to dissect the spatiotemporal evolution of metastatic hepatocellular carcinoma. Cancer Cell 42: 135-156.e17, 2024.
49. Garcia-Lezana T, Lopez-Canovas JL and Villanueva A: Signaling pathways in hepatocellular carcinoma. Adv Cancer Res 149: 63-101, 2021.
50. Cheng X, Yin H, Fu J, Chen C, An J, Guan J, Duan R, Li H and Shen H: Aggregate analysis based on TCGA: TTN missense mutation correlates with favorable prognosis in lung squamous cell carcinoma. J Cancer Res Clin Oncol 145: 1027-1035, 2019.
51. Jiang X, Stockwell BR and Conrad M: Ferroptosis: Mechanisms, biology and role in disease. Nat Rev Mol Cell Biol 22: 266-282, 2021.
52. Zhang C, Liu X, Jin S, Chen Y and Guo R: Ferroptosis in cancer therapy: A novel approach to reversing drug resistance. Mol Cancer 21: 47, 2022.
53. Lee SH, Oh J, Lee ST, Won D, Kim S, Choi HK, Kim SJ, Han H, Yoon M, Choi JR, *et al*: Generation of a human induced pluripotent stem cell line YCMi004-A from a patient with dilated cardiomyopathy carrying a protein-truncating mutation of the titin gene and its differentiation towards cardiomyocytes. Stem Cell Res 59: 102629, 2022.
54. Linke WA and Hamdani N: Gigantic business: Titin properties and function through thick and thin. Circ Res 114: 1052-1068, 2014.
55. Hinson JT, Chopra A, Nafissi N, Polacheck WJ, Benson CC, Swist S, Gorham J, Yang L, Schafer S, Sheng CC, *et al*: HEART DISEASE. Titin mutations in iPS cells define sarcomere insufficiency as a cause of dilated cardiomyopathy. Science 349: 982-986, 2015.
56. Richardson DR and Ponka P: The molecular mechanisms of the metabolism and transport of iron in normal and neoplastic cells. Biochim Biophys Acta 1331: 1-40, 1997.
57. Hassannia B, Vandenabeele P and Vanden Berghe T: Targeting ferroptosis to iron out cancer. Cancer Cell 35: 830-849, 2019.
58. Zou Y, Palte MJ, Deik AA, Li H, Eaton JK, Wang W, Tseng YY, Deasy R, Kost-Alimova M, Dančík V, *et al*: A GPX4-dependent cancer cell state underlies the clear-cell morphology and confers sensitivity to ferroptosis. Nat Commun 10: 1617, 2019.
59. Yang WS, SriRamaratnam R, Welsch ME, Shimada K, Skouta R, Viswanathan VS, Cheah JH, Clemons PA, Shamji AF, Clish CB, *et al*: Regulation of ferroptotic cancer cell death by GPX4. Cell 156: 317-331, 2014.
60. Conrad M and Pratt DA: The chemical basis of ferroptosis. Nat Chem Biol 15: 1137-1147, 2019.
61. Li SH, Mei J, Cheng Y, Li Q, Wang QX, Fang CK, Lei QC, Huang HK, Cao MR, Luo R, *et al*: Postoperative adjuvant hepatic arterial infusion chemotherapy With FOLFOX in hepatocellular carcinoma with microvascular invasion: A multicenter, phase III, randomized study. J Clin Oncol 41: 1898-1908, 2023.
62. Longley DB, Harkin DP and Johnston PG: 5-fluorouracil: Mechanisms of action and clinical strategies. Nat Rev Cancer 3: 330-338, 2003.
63. Herman DS, Lam L, Taylor MR, Wang L, Teekakirikul P, Christodoulou D, Conner L, DePalma SR, McDonough B, Sparks E, *et al*: Truncations of titin causing dilated cardiomyopathy. N Engl J Med 366: 619-628, 2012.